

# Accurately Classifying Out-Of-Distribution Data in Facial Recognition\*

Gianluca Barone<sup>†</sup>, Aashrit Cunchala<sup>‡</sup>, and Rudy Nunez<sup>§</sup>

*Project advisor: Nicole Yang<sup>¶</sup>*

**Abstract.** Standard classification theory assumes that the distribution of images in the test and training sets are identical. Unfortunately, real-life scenarios typically feature unseen data (“out-of-distribution data”) which is different from data in the training distribution (“in-distribution”). This issue is most prevalent in social justice problems where data from under-represented groups may appear in the test data without representing an equal proportion of the training data. This may result in a model returning confidently wrong decisions and predictions. We are interested in the following question: Can the performance of a neural network improve on facial images of out-of-distribution data when it is trained simultaneously on multiple datasets of in-distribution data? We approach this problem by incorporating the Outlier Exposure model and investigate how the model’s performance changes when other datasets of facial images were implemented. We observe that the accuracy and other metrics of the model can be increased by applying Outlier Exposure, incorporating a trainable weight parameter to increase the machine’s emphasis on outlier images, and by re-weighting the importance of different class labels. We also experimented with whether sorting the images and determining outliers via image features would have more of an effect on the metrics than sorting by average pixel value. Our goal was to make models not only more accurate but also more fair by scanning a more expanded range of images. We also tested the datasets in reverse order to see whether a more fair dataset with balanced features has an effect on the model’s accuracy.

**Key words.** Facial recognition, out of distribution data, image detection, machine learning classification

**1. Introduction.** Facial recognition is increasingly being used in the medical, security, and criminal investigation fields, along with many more as time passes. In an attempt to create machine learning models for classifying faces through facial recognition, many large data sets have been collected. However, in many these data sets, there is a heavy representation of Caucasian faces, while other races are underrepresented. As a result, recent studies show that the skew in data sets can be around 80% in favor of lighter skin tones [23]. This leads to situations where models fail to detect darker skin tones. One such example is when Microsoft, IBM, and Face++ classifiers were tested against data sets where it was shown they all performed best on lighter faces, and performed worst on darker female faces [3]. To combat this issue, some data sets have been curated to provide a more balanced division of groups. One such example is that of Fair-face [21], which was developed specifically to provide an equal division of race defined through 7 categories.

The topic of reducing bias to create a fairer model has been widely worked on in recent years, beyond just creating balanced data sets. Particularly, it has been seen that a model can struggle when encountering data with different distributions than the one present in the

\*Submitted to the editors June, 2024.

**Funding:** This work was funded in part by the US NSF award DMS-2051019.

<sup>†</sup>Department of Mathematics, Rowan University, Glassboro, NJ ([barone56@students.rowan.edu](mailto:barone56@students.rowan.edu)).

<sup>‡</sup>Department of Applied Mathematics, University of Pittsburgh, Pittsburgh, PA ([aac130@pitt.edu](mailto:aac130@pitt.edu))

<sup>§</sup>Department of Mathematics, Emory University, Atlanta, GA ([rudy.nunez@emory.edu](mailto:rudy.nunez@emory.edu))

<sup>¶</sup>Department of Mathematics, Emory University, Atlanta, GA ([tianjiao.yang@emory.edu](mailto:tianjiao.yang@emory.edu))

training data. Often, in real-world applications, these distributional differences create issues with the model’s ability to detect minority groups, due to the overpowering amount of a majority group data. One approach to this problem is to instead expose the model to out-of-distribution (OOD) data during the training process, through the use of Outlier Exposure[12]. One potential shortcoming of this method is that in real life, information about the OOD data can not be guaranteed.

The contribution of our paper is

- We compare the advantages between loss re-weighting and Outlier Exposure motivated by their different restrictions on the support of input and output data.
- We modify the Outlier Exposure accordingly in terms of the loss computation and the exposure parameter by taking advantage of the distance between the training and outlier distributions.
- We observe the effects that editing the weighting parameter has on accuracy and observe that our changes results in fewer data points being falsely identified

**2. Distribution Shifts in Classification.** Our focus was on the classification problem in facial recognition. Consider a large-scale facial image dataset containing  $N$  images,  $\{\mathbf{x}_i, y_i\}_{i=1}^N$ , where  $\mathbf{x}_i \in \mathcal{X}$  denotes the  $i$ -th facial image and  $y_i \in \{1, \dots, K\}$  denotes the corresponding label, for example, the identity of the person in the image. The goal of a model is to approximate a function,  $f(x)$ , to relate the images to their labels based on the training samples  $\{\mathbf{x}_i^{\text{train}}, y_i^{\text{train}}\}_{i=1}^n$ . If this relationship is successfully established, then the labels  $y^{\text{test}}$  can be found by  $f(x^{\text{test}})$ . In training, the input images  $\mathbf{x}_1^{\text{train}}, \dots, \mathbf{x}_n^{\text{train}}$  are independent and identically distributed random variables following the image distribution  $P(\mathbf{x})$ . The output labels of training data follow a conditional distribution given  $\mathbf{x}^{\text{train}}$ ,

$$y_i^{\text{train}} \sim P(y|\mathbf{x} = \mathbf{x}_i^{\text{train}}).$$

In standard classification problems,  $x^{\text{train}}$  and  $x^{\text{test}}$  are from identical distributions, however, in our application the two distributions are not the same. Instead, we have the training distribution  $P(x^{\text{train}})$  and testing distribution  $Q(x^{\text{test}})$ .

**2.1. A toy example.** Let’s consider a toy example to see how a typical model can run into classification issue on new or out-of distribution data. Let’s make the classification of the model binary. We have the problem shown as below:

**Example 2.1.** Take input data  $\mathbf{x} = (x_1, x_2)$ , label  $y = \{0, 1\}$ . We first set up an explicit mapping  $f : \mathbf{x} \rightarrow y$ , where

$$(2.1) \quad f(x_1, x_2) = \begin{cases} 1 & \text{if } x_1^2 + x_2^2 \leq 4 \\ 0 & \text{otherwise.} \end{cases}$$

The training data  $(\mathbf{x}^{\text{train}}, y)$  has inputs from the smaller square  $\mathbf{x}^{\text{train}} \in [-1.5, 1.5]^2$ , and  $y = f(\mathbf{x}^{\text{train}})$ . The test data is a uniform mesh grid on  $[-6, 6]^2$ . If the mapping and classification is correct all the area outside the circle should be red. The image below shows that the classification result is accurate for data points close to the given training data. However, the learned function fails to classify the cross-shaped area outside the circle correctly but is confident in making that incorrect prediction. This shows the learning algorithm over-confidently gives wrong classification results on the test data it has not seen before.

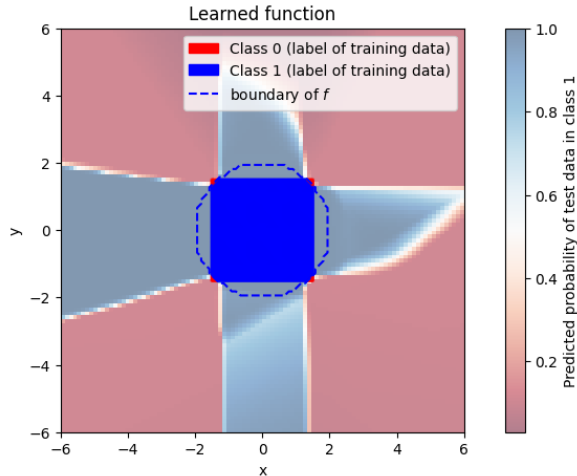


Figure 1: Any point inside the dashed circle gives  $f(\mathbf{x}) = 1$  and its true label is class 1, while the true label of points in the rest of the whole space  $[-6, 6]^2$  is class 0. The color bar on the side gives the predicted probability of the test data (a uniform mesh grid on  $[-6, 6]^2$ ) in class 1.

When the data provided is reliable (truly sampled from  $P_{in}(\mathbf{x}, y)$ ) the classifier gives a good result. In facial recognition problems, out-of-distribution data could appear due to changes in environment, gender, or demographic distributions. These incorrect decisions can have catastrophic consequences. Our paper attempted to resolve this by introducing a form of adjustment for the model known as outlier exposure.

**2.2. Major issues.** There were two major issues we faced when working with this classification problem. The first one was data imbalance. The distributions of different classes in the two datasets were different. FairFace had a near 50/50 split between male and female faces while UTKFace was heavily slanted in favor of male faces. The other major issue we faced was the two datasets being out-of-distribution. As we will show the two datasets had non-overlapping parts which makes it difficult to classify images using typical classification strategies.

To correct the imbalances found within the training and test sets, we attempt weighting the sampling as well as weighting the importance of each sample. Due to the fact that datasets always have an uneven amount of samples between classes, we strengthen the importance of the minority classes to help offset the imbalances. As has been shown (Byrd and Lipton, 2019)[4], given a set of samples in a distribution,  $P(x)$ , and some target distribution,  $Q(x)$ , being approximated by the function,  $f(x)$ , importance sampling would produce an unbiased estimate given by the likelihood ratio  $\frac{Q(x)}{P(x)}$ :

$$(2.2) \quad \mathbb{E}_P \left[ \frac{Q(x)}{P(x)} f(x) \right] = \mathbb{E}_Q[f(x)]$$

For that reason, we focus on weighting the importance according to the likelihood ratio.

In practice, we manually tune the re-scaling weight for each class based on the distribution of training data. The goal of the class reweighting is to show how the model’s performance is affected by out-of distribution data instead of imbalanced distributions.

One of our main approaches is to implement Outlier Exposure with varying datasets to accurately update parameters based on distributions. To do this, we use the Kullback–Leibler (KL) divergence, which quantifies the distributions based on pixel intensity to find the strongest outliers in both datasets. For each dataset, the images are sorted based on their KL distance from the distribution. We collected the 20% of data with the greatest KL distance from each dataset to create an outlier dataset containing the most significant outliers. We then use this new dataset for Outlier Exposure to expose the model to the most significant outliers.

We find that re-weighting and Outlier Exposure both benefit performance, however in some cases one is superior to the other. We find that reweighting balances the model’s predictions for each class, whereas outlier exposure has a greater effect on improving accuracy and other metrics such as precision and recall. However, both techniques can be used simultaneously to compliment each other, but it is important to consider how the weighted classes will affect the predictions made on the Outlier Exposure group. These weights were specified and the formula provided in section 3.4.

### 3. Methods.

**3.1. Explaining Outlier Exposure.** One common way to alleviate out-of-distribution data (OOD) missing their true labels is by using auxiliary out-of-distribution data. This auxiliary data can be incorporated into the model through an OOD-detection score that can then be used to generalize unseen data through the model [12]. The loss function for this model is:

$$(3.1) \quad \min_{\theta} \mathbb{E}_{P_{in}(\mathbf{x},y)}[L(f_{\theta}(\mathbf{x}), y)] + \lambda \mathbb{E}_{P_{out}(\mathbf{x}^{OE}, y^{OE})}[L(f_{\theta}(\mathbf{x}^{OE}), y^{OE})],$$

where  $x$  is an  $1 \times n$  pixel-intensity vector of the in-distribution data,  $y$  is the  $1 \times n$  true-labeling of the images contained in the in-distribution set,  $x^{OE}$  is the  $1 \times n$  pixel-intensity vector of the auxiliary data-set, and  $y^{OE}$  is a  $1 \times n$  vector of the true-labeling of the auxiliary dataset. The first addend is a loss function designed to minimize the loss of the in-distribution data to increase model accuracy. The second add is a loss function, with separate predictions and weights, designed to minimize the loss of out-of-distribution data in the model’s decision making process. The parameter  $\lambda$  is then trained to find the optimal ratio between the weights of the in-distribution and out-of distribution data during each epoch.

To clarify further,

$$(3.2) \quad \mathbb{E}_{P(\mathbf{x},y)}[L(f_{\theta}(\mathbf{x}), y)]$$

is the loss for in-distribution data. It is a product between the expected value of a function of pixel-intensity and true-labeling and the cross-entropy loss function of the pixel-intensity and true-labeling.

$L(\cdot, \cdot)$  is the cross-entropy loss function which measures the distance between the target probability distribution and the learned probability distribution. That is

$$(3.3) \quad \mathbb{E}_{P_{in}(\mathbf{x},y)}L(f_{\theta}(\mathbf{x}), y) = \mathbb{E}_{P_{in}(\mathbf{x},y)}[-\log P_{\theta}(\mathbf{x}, y)].$$

Since images can only belong to one class, the probability of the image belonging to the true label is 1 and so, the probability of the image belong to the other labels are 0. Therefore with  $n$  samples, the expectation can be approximated by  $\frac{1}{n} \sum_{i=1}^n L(f_{\theta}(\mathbf{x}_i), y_i)$ . Therefore our equation changes to

$$(3.4) \quad \begin{aligned} \mathbb{E}_{P_{in}(\mathbf{x},y)} L(f_{\theta}(\mathbf{x}), y) &= \mathbb{E}_{P_{in}(\mathbf{x},y)} [-\log P_{\theta}(\mathbf{x}, y)] \\ &\approx -\frac{1}{n} \sum_{j=1}^n \sum_{i=1}^K \mathbf{1}[y_j = i] \log p_{\theta}(y_j = i | \mathbf{x}_j), \end{aligned}$$

where the distribution  $p_{\theta}(y_j = i | \mathbf{x}_j)$  is learned from a neural network by using the typical softmax function. This process generates the learned probability distribution.

$$(3.5) \quad \mathbb{E}_{P_{out}(\mathbf{x}^{OE})} [L(f_{\theta}(\mathbf{x}^{OE}), y^{OE})]$$

is the loss for Outlier Exposure data. The Outlier Exposure implemented in our model is approximated through:

$$(3.6) \quad OE = -\frac{1}{n} \sum_{j=1}^n \sum_{i=1}^K \mathbf{1}[y_j = i] \log p_{\theta}(y_j = i | \mathbf{x}_j) - \frac{1}{n} \sum_{j=1}^n \sum_{i=1}^K \mathbf{1}[y_j = i] \log p_{\theta}(y_j = i | \mathbf{x}_j).$$

where  $x_j$  is the in-distribution data set, UTKFace,  $y_j$  are the true labeling,  $x_{OE}$  is the out-of-distribution, and  $y_{OE}$  is the true labeling of the out-of-distribution data where the out-of-distribution varies between different datasets. Essentially  $x_{OE}$  is the distribution of the model's class prediction for the test set and  $y_{OE}$  is the true classes for the test set.

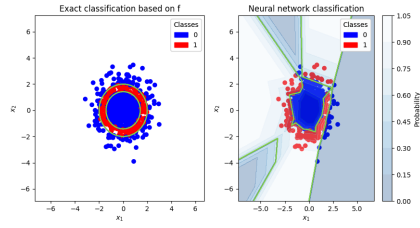
**3.2. Outlier Exposure Toy Example.** This project focuses on improving facial recognition algorithms and seeing their effects on out-of-distribution data. The model has not seen data from  $P_{out}$  during training and consequently that data may be incorrectly identified. The effect can be seen in the images shown below.

As can be seen in Figure 2, outlier exposure does allow for classification to be more accurate for different classes. There are a couple of things to keep in mind when looking at this image. First, the classifier is a simple case and can be defined explicitly as the donut shaped region. In the real world, this relationship is not as trivial. This disparity of difficulty will cause the issue of out-of-distribution data to be more severe in real-world facial recognition applications.

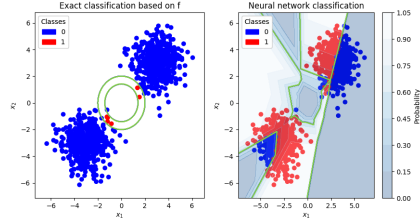
**3.3. Toy examples.** We use simple 2D binary classifications as examples.

**Example 3.1.** Take input data  $\mathbf{x} = (x_1, x_2)$ , label  $y = \{0, 1\}$ . We first set up an explicit mapping  $f : \mathbf{x} \rightarrow y$ , where

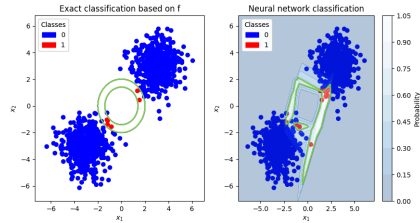
$$(3.7) \quad f(x_1, x_2) = \begin{cases} 1 & \text{if } 2 \leq x_1^2 + x_2^2 \leq 5 \\ 0 & \text{otherwise.} \end{cases}$$



(a) Training and testing on in-distribution data.



(b) Training on in-distribution data, and testing on out-of-distribution data.



(c) Training on in-distribution data, and testing on out-of-distribution data with outlier exposure

Figure 2: **A simple math example to illustrate outlier exposure.** Three pairs of classification results in the toy example. From top to bottom: (a) is the result when training and testing data set is using the same normal distribution (in-distribution data). (b) is training on in-distribution data, and testing on out-of-distribution data. (c) Training on in-distribution data, and testing on out-of-distribution data with outlier exposure

When the data is reliable, that is, when they are truly sampled from  $P_{in}(\mathbf{x}, y)$ , the trained classifier will give a good classification result. Here data  $\mathbf{x}$  in the training and testing stage are both sampled from the same normal distribution.

Now with the training (in-distribution) data sampled from 2D Gaussian distribution, we sample a different test (out-of-distribution) data sampled from a bi-modal Gaussian mixture distribution. One can see that a lot of out-of-distribution data has been incorrectly classified into class 0 and 1. See Figure 2b.

One common way is to use a neural network to approximate  $f$  by  $f_\theta$ . In this example, we used a simple fully-connected neural network with 2 hidden layers and 100 neurons per layer

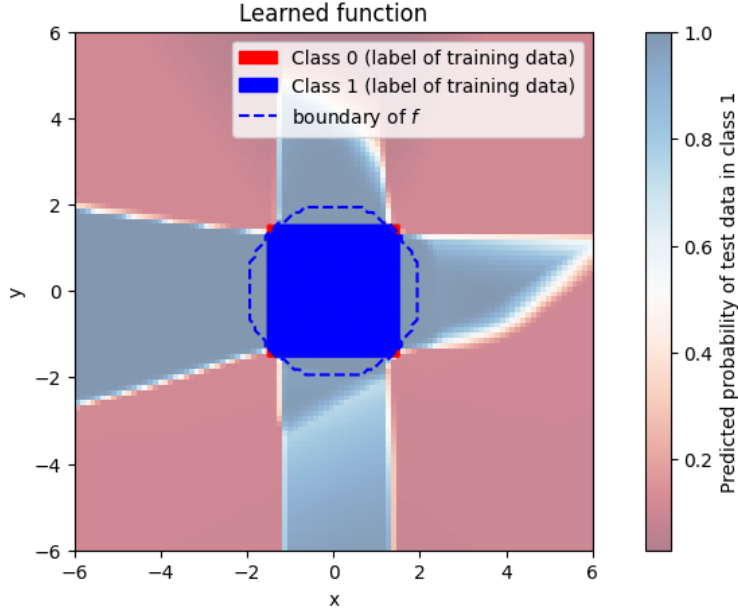


Figure 3: Any point inside the dashed circle gives  $f(\mathbf{x}) = 1$  and its true label is class 1, while the true label of points in the rest of the whole space  $[-6, 6]^2$  is class 0. The training data  $(\mathbf{x}^{\text{train}}, y)$  has inputs from the smaller square  $\mathbf{x}^{\text{train}} \in [-1.5, 1.5]^2$ , and  $y = f(\mathbf{x}^{\text{train}})$ . This can be seen in the middle small square with blue (class 1) in the overlapping part with  $x_1^2 + x_2^2 \leq 4$ ; and red corners (class 0). The color bar on the side give the predicted probability of the test data (a uniform mesh grid on  $[-6, 6]^2$ ) in class 1.

and apply Adam optimizer to optimize the cross-entropy loss.

In facial analysis applications, the out-of-distribution data could appear because of the different environment, such as lighting, or the different demographic or gender distribution during data collection. A face recognition algorithm transforms an image  $\mathbf{x}$  into an output class  $y$  indicating the identity of the person in that image. To train a face recognition model, a dataset needs to have many different images of faces. However if the dataset uses photos taken indoors  $P_{in}(\mathbf{x})$  to train the model, then images from outdoor lighting conditions  $P_{out}(\mathbf{x})$  might cause the model to perform poorly. In another scenario, we want to train an algorithm to recognize personal attributes, such as emotion, from images of faces. People create a dataset of facial images with labels about emotion level sad to happy  $P_{in}(y|\mathbf{x})$ . However cultural difference could result in different labels when a different group of people look at the same set of images  $P_{out}(y|\mathbf{x})$ . This might also result in wrong decisions from the model.

**3.4. Outlier Exposure with An Importance Re-weighting scheme.** One approach we used to account for the out-of distribution data was by weighting the loss function in Equation (3.1). This was done by weighting the first term, the loss for in-distribution data. That

is,

$$(3.8) \quad \mathbb{E}_{P_{in}(\mathbf{x},y)} L(f_{\theta}(\mathbf{x}), y) \approx -\frac{1}{n} \sum_{j=1}^n \sum_{i=1}^K w_i \mathbf{1}[y_j = i] \log p_{\theta}(y_j = i | \mathbf{x}_j),$$

where the weights to use can be found by

$$(3.9) \quad w_i = \frac{n}{2y_i^{\text{train}}}$$

where  $w_i$  is the weight used for the  $i$ th class,  $n$  is the total number of images in a dataset, and  $y_i^{\text{train}}$  is the number of images in the  $i$ th class, for  $i \in [0, 1]$ . Additionally, we primarily used the rescaled weights, where  $w_0 = 1$ , and  $w_1$  is scaled accordingly.

This improves classification as more weight is placed on the positive class, which we consider to be the minority class of females for gender classification. Thus, when the loss function is being optimized, it will be penalized heavier for errors made when training on the minority class.

In order to find the appropriate images for the outlier exposure data we needed to quantify which images were outliers. We started by using the Kullback-Leibler divergence to measure the difference between two probability distributions over a variable  $x$ . The two distributions used were the pixel value distributions obtained from each dataset. This divergence allows us to identify the 20% of images from the UTKFace and FairFace dataset that represent the most significant outliers when compared to the distribution of the UTKFace dataset. These images were then compiled into separate folders to be used in Outlier Exposure testing where we analyze the distribution of each dataset based on the frequency of the pixel values. As seen in the figure below, blue represents the UTKFace dataset and orange represents the FairFace dataset. The  $x$  axis (pixels) are capped at 255 due to the standard RGB scale. Every image in the dataset is a random variable  $\mathbf{x} \in [0, 1]^{n^2}$ , where  $n$  is the resolution value. The pixel average for the current image examined is defined as  $\mathbf{x}_1$  and the overall distribution of pixel averages for all pixels is defined as  $\mathbf{x}_2$ , with the range for each of these averages between 0 to 255. The distance is defined as the distance between  $\mathbf{x}_1, \mathbf{x}_2$  in the defined space. In this case we used the KL divergence which uses probability distributions. In probability distributions  $P$  and  $Q$  it is defined as

$$(3.10) \quad D_{\text{KL}}(P \parallel Q) = \sum_{x \in \mathcal{X}} P(x) \log \left( \frac{P(x)}{Q(x)} \right)$$

The pixel frequency distribution represents the percentage of pixels with a given intensity featured in all images in a given dataset. As can be seen in Figure 4, the mean RGB value of the UTKFace dataset is close to 120, while the mean of the FairFace dataset is closer to 70. Higher mean RGB values suggest that the dataset has brighter or more intense colors relative to lower mean RGB values [34]. From this, we take away that the UTKFace dataset contains brighter images than the FairFace dataset, which might be due to image quality. That is an avenue for future research for classification models.

We also find that the Kullback-Leibler divergence between the two datasets to be 0.088. Smaller KL divergences imply that two datasets are similar [8]. This similarity is supported



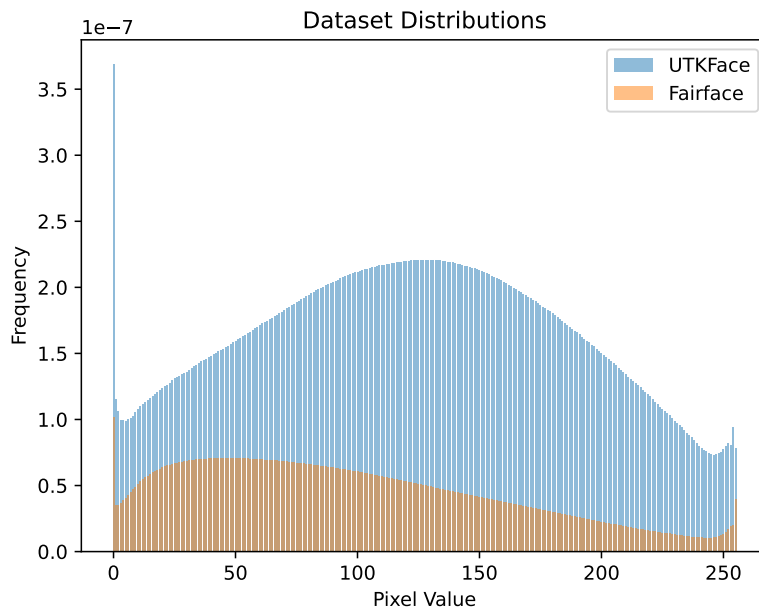


Figure 4: Distribution of Pixel Frequency in UTKFace & FairFace

by Fig. 4, and may lead to issues when using this data in Outlier Exposure models because the two distributions are not at a level of distinction necessary for Outlier Exposure to be impactful [12].

However, there are major issues with comparing datasets using simple pixel values. Pixel values are incredibly sensitive to variation in lighting and are drastically affected by image transformations [15], computationally expensive [32], and do not consider important semantic content such as shapes and textures in an image [6]. In addition, by using pixels we are considering every pixel value in an image, which includes background details that can lead to noisy and/or irrelevant features hindering accurate dataset comparisons [20].

Another method of comparing distributions can be done through activation features. Activation features, also known as feature maps, are the output maps of intermediate layers of a Convolutional Neural Network when the network performs forward propagation [24]. They have several benefits when compared to direct pixel values. Namely, they encode semantic information, reduce dimensionality to make computation more efficient, and are unaffected by image transformations [2]. We found the histogram plots of the activation features for the UTKFace and FairFace datasets. They are shown in the histograms in Fig. 5:

The range of the features in the UTKFace dataset is limited as seen by the constraints of the  $x$ -axis. This range suggests that there is relatively minimal diversity in the contents of the UTKFace dataset. In addition, low activation values suggest that the feature is not abundantly apparent in the input data [14]. The dataset as a whole does not have an activation feature above 0.2, suggesting that none of the features appear in a large number of the input

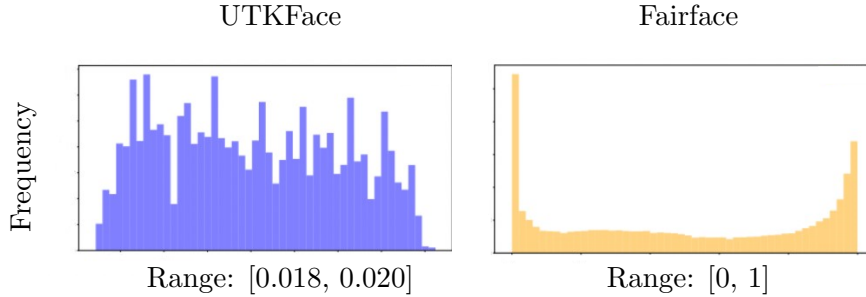


Figure 5: Frequency histogram of activation features in UTKFace and FairFace

images.

Comparatively, the FairFace dataset histogram in Fig. 5 has a remarkably different distribution. A large number of the features are in a similar range as the UTKFace Dataset, but unlike UTKFace, some remain outside that range. This suggests that the distribution of the FairFace dataset may have a bigger spread than that of the UTKFace dataset.

Additionally, this also confirms our belief that the two datasets are not nearly as similar as they appear when compared using pixel value frequencies. In order to quantify the difference between the two datasets we decided to use the Kullback-Leibler divergence. This is important because the Outlier Exposure method of classification is only effective if two datasets have varied distributions.

The Kullback-Leibler divergence for the two datasets when comparing activation features, instead of pixels, was over 2800. A higher KL divergence values suggest that the two datasets are more dissimilar [8].

**3.5. Identifying and Quantifying Outlier Images and Datasets.** After confirming that the two datasets have significantly different distributions, it is important to use this to modify the training of the neural network to classify out-of distribution data. One way of tackling the issue of classification of out-of distribution data is by attempting to shift the distribution of the two datasets together [31]. The hope is that by shifting the distributions closer, the model will better predict the test data as it is closer to the data seen before. To do this we first needed to identify the largest 20% of outliers in both the UTKFace and FairFace dataset; that is, we needed to find the images in each dataset that are farthest from the mean of the dataset. This would also allow us to quantify how far apart the datasets are from each other. This is relevant because if the two distributions are relatively similar, Outlier Exposure may not work[12]. Furthermore, we can use the difference in distributions to modify the  $\lambda$  in (3.1). Although  $\lambda$  was initially fixed to 0.5, we modified it to be function of the distribution differences of the training datasets. The equation for lambda was written as:

$$(3.11) \quad \lambda(D_{\text{KL}}) := \tanh(D_{\text{KL}}),$$

where  $D$  represents the KL pixel distance between the two distributions. This was further modified to change with respect to the number of epochs that have elapsed since training

began in order to have the weight adjusted as the model sees the images more.

$$(3.12) \quad \lambda(D_{\text{KL}}, i) := \tanh(D_{\text{KL}})(1 - \cos(\frac{i\pi}{20}))$$

where  $i$  represents the current epoch from 1 to 20. This iteration causes  $\lambda$  to increase as time passes, which places greater value on the second loss term during the last epochs of the model. In addition to changing  $\lambda$ , we also altered when we calculate the KL distance so to yield different values. Initially, the KL distance of the two full distributions was implemented, then the KL distance of in-distribution and out-of-distribution in batch sizes of 16 images. This was done to see if smaller distributions might reveal intricacies within the dataset that were obscured at a more macro level.

The model was also tested on the CelebA dataset to classify gender. We took five trials of each scenario to get a better average and observe any variation between the models. The results shown in Table 6 are consistent with the ones seen in Table 5, where our improved model performs better in both accuracy and other metrics such as recall and precision.

Due to averaging multiple trials, we also observe the variance and standard deviation between both models. When comparing the values seen in the tables, it can be seen that on average, the standard deviation and variance of the model with outlier exposure is smaller than that of the model without. A lower standard deviation means that the results are less varied and more consistent. When considering results it can be seen that our model with outlier exposures delivers strong performance with consistency, as the variation is small.

## 4. Experiments.

**4.1. Datasets.** One dataset that we primarily use to train our model is the UTKFace dataset [36]. The dataset consists of over 20,000 images labeled by age, gender, and race. Age is labeled numerically from 0-116. For gender, 0 is male, and 1 is female. For race, 0 is White, 1 is Black, 2 is Asian, 3 is Indian, and 4 is for any other races.

We use the FairFace dataset [21] for training and testing, depending on the experiment. This dataset consists of around 100,000 images, and a csv containing the labels for age range, gender, and race. To make our image names in the same format, we use a program to rename all the images in the FairFace folder to match the naming scheme of UTKFace. In addition, race is divided into seven categories, contrasting with UTKFace which has five. To account for this, we assigned White for Middle Eastern, and combined East Asian and Southeast Asian into Asian to mimic how UTKFace labels their images.

CIFAR-10 [19] is also used for the out-of-distribution dataset for Outlier Exposure. This dataset consists of 10 classes of objects consisting of airplane, automobile, bird, cat, deer, dog, frog, horse, ship, and truck. This was chosen as an OOD set since we believe the pictures should appear different when compared to faces.

Labeled Faces in the Wild (LFW) [16] is used to test our model on a different dataset. LFW was used for gender classification. When looking at the gender distribution of this set, there are around 10,000 male images, and around 3,000 female images. It consists of 13,000 images of different famous faces. This dataset was chosen as it is a widely used, large dataset consisting of faces.

CelebA [22] is used similarly to the LFW dataset. The dataset consists of 202,599 images

of celebrities. Although they contain labels for many different traits, only the gender label was used. Unlike LFW, the amount of male and female faces in the dataset is more balanced.

FairFace and UTKFace were also used experimentally as the OOD dataset. For each dataset, one approach was to use the entire dataset as the OOD set. Another approach was through using the outliers to create a smaller dataset consisting of the outliers of either FairFace or UTKFace.

**4.2. Dataset Processing.** The datasets are identified and outliers were sorted using the KL distribution based on pixel values. The program needed to recognize the class for the UTKFace images and the renames FairFace images without an existing csv file of their labels. One of the functions in our class took care of this by sorting through the three variables mentioned in the file name of each image above. In the pre-processing class we also converted the image file path to an RGB array that could be used as an input for the neural network. Other research has previously shown that [28] convolutional neural networks (CNN) perform better on RGB images relative to other forms of deep learning. Finally we need to pre-process the images in order to ensure standard input to the network. As previous work showed [10] neural networks take inputs of the same size and such that the images needed to have a fixed size before being used as inputs to the CNN. The image size we decided on was 32 pixels by 32 pixels, requiring to resize in order to avoid issues with computation time. Images that are modified in size struggle when processed by a neural network [9]. To mitigate this problem we attempt to avoid minimizing images by too large of an amount. The FairFace images were became resized to 32 by 32 and all images were transformed into tensors necessary for CNN image processing. [9]. The tensors were also normalized before going through the network in order to make sure all the images are comparable.

**4.3. Network Infrastructure.** In our model the network is a convolutional neural network (CNN) - a deep learning model for processing data that uses grid patterns [17] designed to learn the spatial hierarchies of different features in the image, making it optimal for facial recognition [7]. There standard CNN contains three layers: convolution, pooling, and fully connected layers. The convolutional and pooling layers extract and process features through applying kernel matrices to preform convolutional and pooling operations. The fully connected layer maps it into an output that can be used for classification [33]. The image below shows an example 6 of how the convolutional network processes the inputted image.

Our first convolutional layer had an input channel of 3 RGB colors, 32 output channels and a kernel size of 5x5 - a common industry standard [13]. Our second layer was a 2x2 kernel size pooling layer used to downsize the sample's spatial dimensions [25] to make the CNN more effective. Average pooling was used (as apposed to max pooling) due to a more representative sample of the pixels in a region. Max pooling becomes skewed towards the dominant pixel features in an image region [35]. We perform a second convolutional layer to extract features from the pooled matrix before being concatenated to an  $1 \times n$  vector and used as an input in the fully connected layers. The fully connected layers use randomly initialized weights to generate probalistic interpretations of the random variable  $x$ , since pictures are loaded into the data loader at random [29]. To extract information from each layer through weight functions the softmax activation function normalizes the output of the loss function so that back propagation can occur to update the randomly initialized weights. As the loss gets

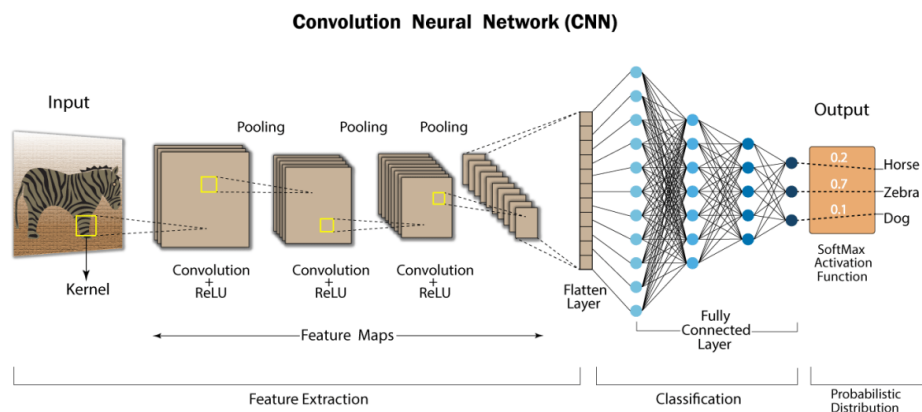


Figure 6: How a CNN Processes an Image.

minimized the weights should converge to the desired function for how to interpret the input. This is done for any given amount of epochs, where finally, the final softmax interpretation will be directly used to produce an label. The amount of outputs matches the size of true-labels in classification. There is also a forward pass function in the class of our neural network that serves to push the image through the different layers of the network mentioned above. The choice was made to use the tanh activation function over the ReLU activation function due to the non-linearity of tanh and its symmetry around zero [26]. The function then returns the image after all the processing was complete.

We pretrained a reasonable convolutional neural network model by testing on in-distribution data. This was to make sure that we can explicitly address our proposed methods on improving the classification of out-of-distribution data.

When testing on in-distribution data, a model generally is able to have the highest accuracy. This is because when the two distributions of training and testing match, the model is well prepared for classifying those images.

As can be seen in Figure ??, when the model is trained and tested on the same distribution, the scores in all main metrics are incredibly high. Interestingly, the same model on FairFace does perform slightly worse, however the images in FairFace are often not as clear as the ones in UTKFace, so it may be harder to classify.

**4.4. Training.** For training, every model was run with 20 epochs to compensate for large computation times. The optimizer we use was the ADAM optimizer [18]. This optimizer was chosen over stochastic gradient descent because we found that it often converged more quickly while having the same loss values.

**4.5. Testing on Out of Distribution Data.** To implement outlier exposure, it requires an in distribution and out-of-distribution dataset. We typically use UTKFace as our in distribution dataset, which gets used as it would in a standard machine learning model. As seen in (3.3), the in distribution data passes through a standard loss function, which was typically cross entropy. The outlier exposure group was varied between different tests. As seen in

(3.5), the outlier group does not pass through a typical loss function as the data for that group does not contain labels but only pictures. To account for this, we added on a second loss function in the code which computes the cross entropy from a softmax distribution to a uniform distribution. This serves to minimize the program’s confidence when predicting the out-of-distribution data, which should help prevent it from being overconfident when encountering other out-of-distribution data when testing. Potential future testing could involve a way for us to improve the weighting schemes by trying to mitigate the weight degeneracy in other ways. We were able to identify the weights of the two classes used in outlier exposure by using 2.2 in order to make sure that our training set was not unduly biased towards male figures.

In general, even if a model had been shown to be adept at recognizing images in the training distribution and accurately classifying them during testing, these results often do not generalize to out-of-distribution data. This meant that we would train the model on one dataset, UTKFace for example, before testing on a different dataset - the goal being able to accurately detect out of distribution. It has been shown that this outcome is incredibly difficult for models since, although they may have a high confidence, their accuracy drops when tested on a different dataset’s distribution [11].

<i>Train Dataset</i>	<i>Test Dataset</i>	<i>Precision</i>	<i>Recall</i>	<i>Accuracy</i>	<i>F1</i>	<i>AUROC</i>
UTKFace	FairFace	0.65	0.68	0.69	0.66	0.77
FairFace	UTKFace	0.87	0.86	0.87	0.86	0.95

Table 1: Results from training and testing on OOD data based on gender. The model being used is tuned for in-distribution data, where all metrics are above 0.97 for UTKFace and 0.91 for FairFace.

The AUROC value of a model trained on UTKFace and tested on FairFace is substantially lower than when it is trained on Fairface and tested on UTKFace. This disparity is due to two major reasons. First, the FairFace dataset has more images which gives the model more data points to learn, which increases the accuracy of the model[13]. Second, the FairFace dataset is also more balanced than the UTKFace data [30] which leads to better accuracy. Those two changes make the FairFace dataset a better training dataset than the UTKFace dataset.

<i>Outlier Group</i>	<i>Precision</i>	<i>Recall</i>	<i>Accuracy</i>	<i>F1</i>	<i>AUROC</i>
None	<b>0.65</b>	0.68	0.69	<b>0.66</b>	<b>0.77</b>
FairFace	0.53	0.52	0.55	0.52	0.60
UTKFace Outliers	0.61	<b>0.71</b>	<b>0.70</b>	<b>0.66</b>	0.75
FairFace Outliers	0.58	0.66	0.66	0.62	0.70
CIFAR-10	0.58	<b>0.71</b>	0.69	0.64	0.75

Table 2: Results from Outlier Exposure when classifying based on gender, training on UTK-Face and testing on Fairface

**4.6. Improving Out-of-Distribution Classification.** We found that the significance of the outlier group had a strong impact on the performance of the model. We believe UTKFace and UTKFace outliers did well due to the change in the distribution of UTKFace becoming more balanced, and potentially bring the distribution between the train and test set closer. However, it seemed that the original model without Outlier Exposure performed better. As seen in Figure 4, the distributions are already similar, providing an explanation to why Outlier Exposure did not work as well as we expected.

In order to improve the results here we used both weighted sample and weighted loss separately in order to observe their effects. In an attempt to take into account the differences in distributions between datasets, the samplings used can be weighted. One approach we use is by taking the Outlier Exposure groups we created earlier from the 20% with the greatest KL divergence and adding that to the training data. This would result in the model being exposed to a larger quantity of outliers to hopefully allow it to classify the images better during testing.

<i>Outlier Sample</i>	<i>Precision</i>	<i>Recall</i>	<i>Accuracy</i>	<i>F1</i>	<i>AUROC</i>
None	0.65	0.68	0.69	0.66	0.77
UTKFace Outliers	0.70	0.68	0.70	0.69	0.77
FairFace Outliers	<b>0.75</b>	<b>0.81</b>	<b>0.80</b>	<b>0.78</b>	<b>0.85</b>

Table 3: Results of increasing the samples for training while training on UTKFace and testing on FairFace

As seen in Table 3, when the model is exposed to an increased sample size it performs much better than without.

Another approach to account for these differences can be by weighing the loss function to pay more attention to one class over another. This is useful in preventing a majority class from overwhelming the minority class. In particular, for gender we weigh the female class higher than the male class. In order to observe this effect we did not implement outlier exposure. Our model was trained on UTKFace and tested on FairFace in order to observe the effect that the weighted sampling had independently on the model.

<i>Male Weight</i>	<i>Female Weight</i>	<i>Precision</i>	<i>Recall</i>	<i>F1</i>	<i>AUROC</i>
1.0	1.0	0.57	<b>0.65</b>	0.61	<b>0.70</b>
1.0	1.5	<b>0.62</b>	0.64	<b>0.63</b>	<b>0.70</b>

Table 4: Results of modifying the weights of loss for male and female classes

As seen in Table 4, we see that increasing the weights of the female class to 1.5 increases the precision while barely decreasing the recall. This means that overall, the model is classifying males and females with around the same accuracy as can be found in the corresponding confusion matrix.

**5. Main results.** We test our model on separate datasets, which simulates a scenario similar to a realistic application. We observe that by adding an outlier group, as outlined in Section 3.4, and weighting the sampling, as described in Section 3.9, that the model performs better than without. We see that even when the extra outlier group is from a different sample entirely, the model is better at adapting to new situations.

<i>Training Group</i>	<i>Precision</i>	<i>Recall</i>	<i>Accuracy</i>	<i>F1</i>	<i>AUROC</i>
FairFace	0.46 ± 0.04	0.26 ± 0.01	0.60 ± 0.02	0.33 ± 0.01	0.57 ± 0.01
FairFace w/ OE	<b>0.54 ± 0.01</b>	<b>0.30 ± 0.01</b>	<b>0.61 ± 0.02</b>	<b>0.38 ± 0.01</b>	<b>0.60 ± 0.02</b>

Table 5: Averaged results from testing on LFW when classifying based on gender, in the form of mean ± standard error

Since there is a strong imbalance between the male and female class in LFW, the loss is weighted by Equation (3.9), using a male class weight of 1 and female class weight of 1.3.

When finding the metrics, the female class was treated as the positive class, which in all prior datasets meant that measuring our accuracy metrics on the male or female class would yield similar values due to the balance between men and women in each set. However, in LFW there are around 10,000 males and 3,000 females, and as such, the metrics seem much lower as there is much less data for women. Regardless, as can be seen in Table 5, our new model performs significantly better than the model that exclusively trains on FairFace. We took the average over five trials to observe any variance in both model. From these averages, it can be seen that there are improvements specifically in precision and recall, which show that a greater percentage of women were accurately predicted.

When comparing the ROC curves for the two experiments, without outlier exposure the AUC is 0.58. This is barely better than randomly guessing, as that would correspond to an AUC of 0.5. Comparatively, with our model the AUC is 0.67, which is a significant jump above the initial model.

An advantage of measuring the average over multiple trials is that the standard error can be found, which shows how much each model varied between tests. When comparing the values seen in Table 5, the smallest standard error in each metric is split between the two models. However, the standard error for precision is much smaller in the model with outlier exposure when compared to the model without.

<i>Training Group</i>	<i>Precision</i>	<i>Recall</i>	<i>Accuracy</i>	<i>F1</i>	<i>AUROC</i>
FairFace	0.59 ± 0.020	0.61 ± 0.007	0.55 ± 0.007	0.60 ± 0.009	0.57 ± 0.008
FairFace w/ OE	<b>0.62 ± 0.007</b>	<b>0.64 ± 0.007</b>	<b>0.58 ± 0.008</b>	<b>0.63 ± 0.005</b>	<b>0.59 ± 0.008</b>

Table 6: Averaged Results from testing on CelebA when classifying based on gender

Similarly to the LFW dataset, we set the weights for the male and female class to 1 and 1.15 respectively.

The model was also tested on the CelebA dataset to classify gender. We took five trials of each scenario to get a better average and observe any variance with the models. The results



shown in Table 6 are consistent with the ones seen in Table 5, where our improved model performs better in both fairness and accuracy.

Due to averaging multiple trials, we also observe the standard error between both models. When comparing the values seen in Table 6, it can be seen that on average, the standard error of the precision of the model with outlier exposure is smaller than that of the model without. A lower standard error means that the results are less varied and more consistent.

Over the course for all experiments, we found that in general, our approach helps to reduce false negatives and false positives. This can be seen by observing the recall and precision in Table 5 and Table 6, in which both fairness metrics increase with our model. As such, this correlates to a lower false negative and false positive rate, which is very important as different applications suffer more from different false rates. In contrast to the healthcare application mentioned above, false positives can be particularly problematic in law enforcement applications, where a subject could be mislabeled as the culprit for a crime they did not commit. As such, being able to reduce both false negative rates is important.

**6. Conclusions.** In this paper, we explore the concept of facial recognition classification. Specifically, we focus on how models struggle when confronted with data from different distributions during training and testing. Out-of-distribution data has been shown to significantly reduce the accuracy of facial recognition models. Throughout this paper, we document the results of a CNN model on different training and testing datasets. We also use KL distribution to identify outlier images from each dataset and incorporate Outlier Exposure into our model to see how it affected the model’s accuracy and other metrics. We also attempt to weight the sampling of the different classes (male and female) and observe how the model’s results change. Overall, we examine how facial recognition models tested on out-of-distribution data and different ways to increase accuracy and other metrics of the model. With the use of artificial intelligence and facial recognition in sectors such as law enforcement and healthcare, the lack of fairness and accurate classification of out-of-distribution data (often data & images of minority groups) has become an increasingly pressing issue. The goal of this paper is to examine different ways through which we can increase the metrics of these models in order to make real-world facial recognition models more fair.

**6.1. Related & Future Work.** While this paper was a good overview of current methods, there are alternate avenues that future researchers may want to explore to increase accuracy. One method is Geometric Sensitivity Decomposition, which works with feature norms of images after they have run through a neural network. Besides the importance weighting and outlier exposure perspectives we looked into, another region of focus is through bringing the distributions of the train and test datasets closer through the modification of the distributions. One such example is [1], where they find fairness can be improved through transforming images of the training data distribution to match that of the test dataset. Other methods also involve modifying the loss function used or devising different ways to weight classes in order to increase accuracy. Along the same lines of fairness transfer, [27] develops a causal approach using conditional independence tests to characterize distribution shifts in healthcare machine learning, revealing that understanding such shifts can diagnose fairness discrepancies and suggesting potential mitigation strategies throughout the ML pipeline. The unfairness that arises from the shift between distributions is becoming widely studied, such as by [5],

where they find that even when a set is balanced, it may favor one group, such as males, so it is not enough to just balance one dataset. One key takeaway is that class imbalances are not the only cause for bias. Our model attempts to account for this by not just using a balanced dataset like FairFace, but also including a secondary outlier dataset to increase fairness.

**Acknowledgments.** We would like to thank our mentor, Dr. Nicole Yang. This work was supported in part by the US NSF award DMS-2051019.

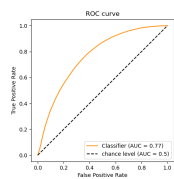
**Appendix A. Definition of Relevant Evaluation Metrics.** Here we define the metrics we used to evaluate our model. Due to the emphasis on the fairness of the model, we evaluated performance based on the confusion matrix and AUROC score. Through the use of the confusion matrix we find precision, recall, accuracy, and F1, with our goal being to maximize each metric, along with the AUROC score. Precision and recall can be calculated using the true positive,  $TP$ , false positive,  $FP$ , and false negative,  $FN$ , where

$$\text{Precision} = \frac{TP}{TP + FP}$$

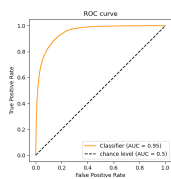
$$\text{Recall} = \frac{TP}{TP + FN}$$

Additionally, the F1 score is the harmonic mean between precision and recall. The area under the ROC curve (AUROC) is a measure of performance, where a model with perfect predictions would have a score of 1, and a model that was always incorrect would have a score of 0.

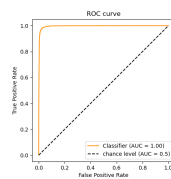
Appendix B. ROC Curves for Experiments.



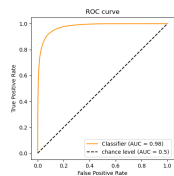
(a) UTKFace-FairFace



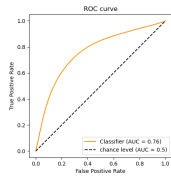
(b) FairFace-UTKFace



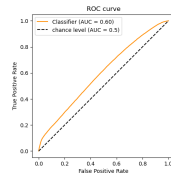
(c) UTKFace-UTKFace



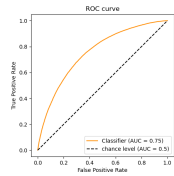
(d) FairFace-FairFace



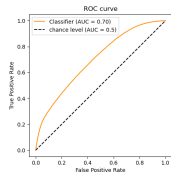
(e) UTKFace-FairFace-UTKFace



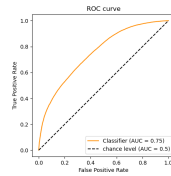
(f) UTKFace-FairFace-FairFace



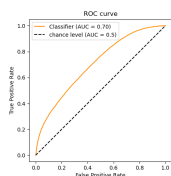
(g) UTKFace-FairFace-UTKFace Outliers



(h) UTKFace-FairFace-Fairface Outliers



(i) UTKFace-FairFace-CIFAR-10



(j) UTKFace-FairFace when loss weights are 1 for male, 1.5 for female

Figure 7: ROC Curve from all experiments used, labelled in the order of "train set-test set-outlier set".

**Appendix C. Confusion Matrix for Experiments.**

<i>Train-Test-Outlier</i>	<i>Male-Male</i>	<i>Male-Female</i>	<i>Female-Male</i>	<i>Female-Female</i>
UTKFace-FairFace	33711	14274	12274	26484
FairFace-UTKFace	10818	1477	1573	9837
UTKFace-UTKFace	12079	226	312	11088
FairFace-FairFace	42657	3754	3328	37004
UTKFace-FairFace-UTKFace	36306	15304	9679	25454
UTKFace-FairFace-FairFace	26010	19041	19975	21717
UTKFace-FairFace-UTKFace Outliers	35693	16079	10292	24679
UTKFace-FairFace-FairFace Outliers	33636	16952	12349	23806
UTKFace-FairFace-CIFAR-10	36486	17144	9499	23614
UTKFace-FairFace (weights 1-1.5)	32003	15503	13982	25255

Table 7: Confusion Matrices from all experiments used. Columns labeled by "Predicted Label-Actual Label"

**Appendix D. KL Divergence Time of Calculations.**

<i>KL Calculation Period</i>	<i>Precision</i>	<i>Recall</i>	<i>Accuracy</i>	<i>F1</i>	<i>AUROC</i>
Full distribution	0.75	0.81	0.80	0.78	0.86
During each iteration	0.76	0.78	0.79	0.77	0.81

Table 8: Results from changing the time at which the KL distribution is calculated

**REFERENCES**

- [1] B. AN, Z. CHE, M. DING, AND F. HUANG, *Transferring fairness under distribution shifts via fair consistency regularization*, 2023.
- [2] S. AZAM, S. MONTAHA, K. U. FAHIM, A. R. H. RAFID, M. S. H. MUKTA, AND M. JONKMAN, *Using feature maps to unpack the cnn ‘black box’ theory with two medical datasets of different modality*, *Intelligent Systems with Applications*, 18 (2023), p. 200233.
- [3] J. BUOLAMWINI AND T. GEBRU, *Gender shades: Intersectional accuracy disparities in commercial gender classification*, in *Conference on fairness, accountability and transparency*, PMLR, 2018, pp. 77–91.
- [4] J. BYRD AND Z. LIPTON, *What is the effect of importance weighting in deep learning?*, in *International conference on machine learning*, PMLR, 2019, pp. 872–881.
- [5] V. CHEREPANOVA, S. REICH, S. DOOLEY, H. SOURI, M. GOLDBLUM, AND T. GOLDSTEIN, *A deep dive into dataset imbalance and bias in face identification*, 2022.
- [6] J. DUAN AND C.-C. J. KUO, *Bridging gap between image pixels and semantics via supervision: A survey*, *ArXiv*, abs/2107.13757 (2021).
- [7] K. FUKUSHIMA, *Neocognitron: A self-organizing neural network model for a mechanism of pattern recognition unaffected by shift in position*, *Biological Cybernetics*, 36 (1980), pp. 193–202.
- [8] S. GALBRAITH, J. A. DANIEL, AND B. VISSSEL, *A study of clustered data and approaches to its analysis*, *The Journal of Neuroscience*, 30 (2010), pp. 10601–10608.
- [9] M. HASHEMI, *Enlarging smaller images before inputting into convolutional neural network: zero-padding vs. interpolation*, *Journal of Big Data*, 6 (2019).

- [10] M. HASHEMI, *Web page classification: A survey of perspectives, gaps, and future directions*, *Multimedia Tools Appl.*, 79 (2020), p. 11921–11945.
- [11] D. HENDRYCKS AND K. GIMPEL, *A baseline for detecting misclassified and out-of-distribution examples in neural networks*, in *International Conference on Learning Representations*, 2017.
- [12] D. HENDRYCKS, M. MAZEIKA, AND T. DIETTERICH, *Deep anomaly detection with outlier exposure*, arXiv preprint arXiv:1812.04606, (2018).
- [13] D. HIRAHARA, E. TAKAYA, T. TAKAHARA, AND T. UEDA, *Effects of data count and image scaling on deep learning training*, *PeerJ Computer Science*, 6 (2020), p. e312.
- [14] J. P. HORWATH, D. N. ZAKHAROV, R. MÉGRET, AND E. A. STACH, *Understanding important features of deep learning models for segmentation of high-resolution transmission electron microscopy images*, *npj Computational Materials*, 6 (2020).
- [15] C. HU, B. B. SAPKOTA, J. A. THOMASSON, AND M. V. BAGAVATHIANNAN, *Influence of image quality and light consistency on the performance of convolutional neural networks for weed mapping*, *Remote Sensing*, 13 (2021).
- [16] G. B. HUANG, M. RAMESH, T. BERG, AND E. LEARNED-MILLER, *Labeled faces in the wild: A database for studying face recognition in unconstrained environments*, Tech. Rep. 07-49, University of Massachusetts, Amherst, October 2007.
- [17] D. H. HUBEL AND T. N. WIESEL, *Receptive fields and functional architecture of monkey striate cortex*, *The Journal of Physiology*, 195 (1968), pp. 215–243.
- [18] D. P. KINGMA AND J. BA, *Adam: A method for stochastic optimization*, 2017.
- [19] A. KRIZHEVSKY, G. HINTON, ET AL., *Learning multiple layers of features from tiny images*, (2009).
- [20] A. KRIZHEVSKY, I. SUTSKEVER, AND G. E. HINTON, *Imagenet classification with deep convolutional neural networks*, in *Advances in Neural Information Processing Systems*, F. Pereira, C. Burges, L. Bottou, and K. Weinberger, eds., vol. 25, Curran Associates, Inc., 2012.
- [21] K. KÄRKKÄINEN AND J. JOO, *Fairface: Face attribute dataset for balanced race, gender, and age*, 2019.
- [22] Z. LIU, P. LUO, X. WANG, AND X. TANG, *Deep learning face attributes in the wild*, in *Proceedings of International Conference on Computer Vision (ICCV)*, December 2015.
- [23] M. MERLER, N. RATHA, R. S. FERIS, AND J. R. SMITH, *Diversity in faces*, 2019.
- [24] L. NANNI, S. BRAHNAM, M. PACI, AND S. GHIDONI, *Comparison of different convolutional neural network activation functions and methods for building ensembles for small to midsize medical data sets*, *Sensors*, 22 (2022), p. 6129.
- [25] R. NIRTHIKA, S. MANIVANNAN, A. RAMANAN, AND R. WANG, *Pooling in convolutional neural networks for medical image analysis: a survey and an empirical study*, *Neural Computing and Applications*, 34 (2022), pp. 5321–5347.
- [26] T. D. RYCK, S. LANTHALER, AND S. MISHRA, *On the approximation of functions by tanh neural networks*, *Neural Networks*, 143 (2021), pp. 732–750.
- [27] J. SCHROUFF, N. HARRIS, S. KOYEJO, I. M. ALABDULMOHSIN, E. SCHNIDER, K. OPSAHL-ONG, A. BROWN, S. ROY, D. MINCU, C. CHEN, ET AL., *Diagnosing failures of fairness transfer across distribution shift in real-world medical settings*, *Advances in Neural Information Processing Systems*, 35 (2022), pp. 19304–19318.
- [28] L. SHAO, Z. CAI, L. LIU, AND K. LU, *Performance evaluation of deep feature learning for rgb-d image/video classification*, *Information Sciences*, 385–386 (2017), pp. 266–283.
- [29] M. M. TAYE, *Theoretical understanding of convolutional neural network: Concepts, architectures, applications, future directions*, *Computation*, 11 (2023), p. 52.
- [30] Q. WEI AND R. L. DUNBRACK, *The role of balanced training and testing data sets for binary classifiers in bioinformatics*, *PLoS ONE*, 8 (2013), p. e67863.
- [31] K. WEISS, T. M. KHOSHGOFTAAR, AND D. WANG, *A survey of transfer learning*, *Journal of Big Data*, 3 (2016).
- [32] F. XING, Y. XIE, X. SHI, P. CHEN, Z. ZHANG, AND L. YANG, *Towards pixel-to-pixel deep nucleus detection in microscopy images*, *BMC Bioinformatics*, 20 (2019).
- [33] R. YAMASHITA, M. NISHIO, R. K. G. DO, AND K. TOGASHI, *Convolutional neural networks: an overview and application in radiology*, *Insights into Imaging*, 9 (2018), pp. 611–629.
- [34] S. ZABALA-TRAVERS, M. CHOI, W.-C. CHENG, AND A. BADANO, *Effect of color visualization and display hardware on the visual assessment of pseudocolor medical images*, *Medical Physics*, 42 (2015),

- pp. 2942–2954.
- [35] A. ZAFAR, M. AAMIR, N. M. NAWI, A. ARSHAD, S. RIAZ, A. ALRUBAN, A. K. DUTTA, AND S. ALMOTAIRI, *A comparison of pooling methods for convolutional neural networks*, Applied Sciences, 12 (2022), p. 8643.
- [36] Z. ZHANG, Y. SONG, AND H. QI, *Age progression/regression by conditional adversarial autoencoder*, in IEEE Conference on Computer Vision and Pattern Recognition (CVPR), IEEE, 2017.